

THERMOPHYSICAL PROPERTIES
OF BINARY AND TERNARY FLUID MIXTURES
FROM DYNAMIC LIGHT SCATTERING¹

A. P. Fröba², S. Will³, and A. Leipertz^{2,4}

-
- ¹ Paper presented at the Fourteenth Symposium on Thermophysical Properties, June 25-30, 2000, Boulder, Colorado, U.S.A.
- ² Lehrstuhl für Technische Thermodynamik (LTT), Friedrich-Alexander-Universität Erlangen-Nürnberg, Am Weichselgarten 8, D-91058 Erlangen, Germany
- ³ Technische Thermodynamik / Wärme- und Stofftransport (TTWSt), Universität Bremen, FB4, Badgasteiner Straße 1, D-28359 Bremen, Germany
- ⁴ Author to whom correspondence should be addressed.

ABSTRACT

Several thermophysical properties of R507, a binary refrigerant mixture, and R404A, a ternary mixture, have been determined by dynamic light scattering (DLS), both in the liquid and in the vapor state along the saturation line approaching the vapor-liquid critical point. Data for the thermal diffusivity a and sound velocity c_s cover a range of temperatures down to 270 K and for the surface tension σ and kinematic viscosity ν down to 230 K. For both mixtures the behavior of all properties determined can well be correlated by the mass weighted sum of respective pure component data, when all data are represented as function of the reduced temperature

KEY WORDS: binary mixture, dynamic light scattering; kinematic viscosity; R507; R404A; ternary mixture, thermal diffusivity; sound velocity; surface tension.

1. INTRODUCTION

Dynamic light scattering (DLS) is a unique diagnostic tool for the determination of a variety of thermophysical properties of fluids using a basically identical experimental setup [1-4]. In pure fluids, the thermal diffusivity can be found from the linewidth of the Rayleigh component of the spectrum of scattered light which arises from entropy fluctuations [5-7]. In binary fluid mixtures, the thermal diffusivity and the mutual diffusivity can basically be determined simultaneously from the linewidth of the Rayleigh line, governed by microscopic fluctuations of temperature and concentration [8-10]. Additionally, both for pure fluids and for fluid mixtures, information about sound velocity and sound attenuation can be obtained from the Brillouin lines of the spectrum, which are shifted in frequency with respect to the incident light and which are caused by pressure fluctuations [4, 11-13]. Information about surface tension and kinematic viscosity can be derived from light scattering at the surface waves, which are caused by the thermal movement of molecules resulting in so-called „ripples“ [4, 14]. For selected fluids, also the dynamic viscosity can be determined by seeding the liquid with small spherical particles of known size [15] which sometimes is even possible simultaneously with other properties, e.g., with the mutual diffusion coefficient in binary liquid systems [16].

Apart from research proving the applicability of the measurement technique itself, investigations of fluid mixtures are quite rare and have – to the best of our knowledge - so far been restricted to binary mixtures [8-10, 17]. In the present paper, for the first time also ternary mixtures have been studied using the DLS technique. Measurements in the binary system R507 (R125 50% wt. / R143a 50% wt.) and in the ternary mixture R404A (R125 44% wt. / R143a 52% wt. / R134a 4% wt.) have been

performed in order to study the behavior of the saturated fluid mixtures when approaching the vapor-liquid critical point. For both the liquid and the vapor phase, thermal diffusivity and sound velocity have been measured by light scattering from the bulk fluid, and liquid viscosity and surface tension have been determined by surface light scattering.

Whether it is possible to determine simultaneously signals from concentration and temperature fluctuations is mainly restricted by the relative difference of the refraction indices of the mixture components and their concentration. However, for the fluid mixtures studied in this work the refractive indices of the pure components have comparable values [18-20] so that from the Rayleigh component of scattered light only a signal from temperature fluctuations associated with thermal diffusivity could be resolved.

2. METHOD AND EXPERIMENTAL SETUP

In contrast to conventional methods, most of which are working with macroscopic gradients according to the desired quantities, DLS provides information on thermophysical properties of fluids in macroscopic thermodynamic equilibrium. The principle of the DLS techniques for the determination of these properties is given in some detail elsewhere (see, e.g., Refs. 1-4 and 21). In these investigations light scattering from bulk fluids provides information on thermal diffusivity and sound velocity and light scattering from surface waves information on surface tension and kinematic viscosity.

The optical and electro-optical parts of the experimental setup used for the determination of sound velocity and thermal diffusivity are shown - in a top view - in

Fig. 1a. For performing light scattering from bulk fluids, the scattering volume, which is determined by the intersection of the incident beam and the axis of observation (dashed line), is located in the middle of the vessel. The principle of the scattering geometry which allows scattering by surface waves is shown schematically - in a front view - in Fig. 1b. In this case, the detected scattering volume is located at the interface between the liquid and vapor phase under saturation conditions. The only modification of the set-up in Fig. 1a for the realization of surface light scattering experiments was to mount the pressure vessel in a vertical position.

As a light source an argon ion laser ($\lambda_0 = 488 \text{ nm}$) or a frequency doubled continuous wave Nd:YVO₄-laser ($\lambda_0 = 532 \text{ nm}$) were optionally used. The laser-power was up to 300 mW when working far away from the critical point, and only a few mW in the critical region. For the determination of sound velocity, a reference beam shifted in frequency by an opto-acoustic modulator was added to the scattered light. Scattered light was detected by two photomultiplier tubes (PMT's), and the cross-correlation function was calculated by a digital correlator. A more detailed description of the experimental set-up can be found in Ref. 4.

According to the specifications of the manufacturer (Solvay) both refrigerant mixtures had a purity of $\geq 99.5\%$ and were used without further purification. The uncertainty in the composition for the binary mixture R507 is certified for each component with $\pm 1\%$ wt.. For the ternary mixture R404A, the uncertainties in the composition are $\pm 2\%$ wt. for R125, $\pm 1\%$ wt. for R143a, and $\pm 2\%$ wt. for R134a. For the present measurements, the samples were filled into a cylindrical pressure vessel (volume $\approx 10 \text{ cm}^3$) from the liquid phase to avoid decomposition in particular for the refrigerant R404A which represents only a near-azeotropic mixture.

The temperature of the pressure vessel, which is placed inside an insulated housing is regulated through resistance heating and measured by calibrated 25-*W* or 100-*W* platinum resistance probes with an uncertainty of ± 0.015 K. The temperature stability was better than ± 0.002 K during one experimental run. For each temperature point, typically six measurements at different angles of incidence have been performed. For temperatures below room temperature, the insulating housing was cooled down to about 10 K below the desired temperature in the sample cell by a lab thermostat.

3. RESULTS AND DISCUSSION

3.1. Binary Mixture R507

The experimental results of the thermal diffusivity and the sound velocity of R507 are displayed in Fig. 2 and 3, respectively. The uncertainties of the measured mixture data for the thermal diffusivity and sound velocity can be estimated to be below $\pm 1\%$ and $\pm 0.5\%$, respectively. In both figures the saturated vapor data are represented by filled symbols and the saturated liquid data by open ones. Additionally, the pure component data of R125 and of R143a are given by dotted and dashed lines, respectively. The pure component data for R125 have been taken from former measurements [22], those for R143a have been measured in the course of this investigation and are reported separately [23]. The data are shown as a function of the reduced temperature

$$T_R = T/T_C \quad (1)$$

using the critical temperature $T_C = 344.06$ K we have found in our measurements by the observation of the vanishing meniscus between liquid and vapor phase when

approaching the critical point. In order to predict the mixture data on basis of the pure component data within the range investigated we have tried several different approaches using, e.g., a simple weighting by the mass fractions or the mole fractions of the pure components. In all these cases, remarkable deviations appeared in the vicinity of the critical point when drawing the data against the temperature. Using, however, the reduced temperature as shown in Fig. 2 and 3 an excellent agreement was found between the measured data and the predicted ones when weighting with the mass fractions w_i as indicated in the figures by the drawn line. The agreement was not this good when using the mole fractions. The data of the drawn line have thus been calculated by, e.g., for the thermal diffusivity a_M of the mixture according to

$$a_M(T_R) = \sum_i w_i a_i(T_R) \quad (2)$$

with the thermal diffusivities of the pure components at the reduced temperature T_R and mass fractions w_i . For the sound velocity the same procedure has been used. As can be seen from the deviation plots in Fig. 2 and 3, the prediction is very good with deviations smaller than 1.5% for the sound velocity mixture data (even smaller than 1% for the liquid phase) and smaller than 4-6% for the thermal diffusivity mixture data (or even smaller than 2% for the liquid phase up to a reduced temperature of about 0.98).

From surface light scattering surface tension and liquid kinematic viscosity have also been measured under saturation conditions. The results of these measurements - together with pure component data, which also have been measured in this study - are displayed in Fig. 4 and 5 for the kinematic viscosity and the surface tension, respectively, again as function of the reduced temperature. For the kinematic viscosity and surface tension besides the mixture data also the pure component data of R125 and

R143a are represented by different symbols. The mixture results for the kinematic viscosity and surface tension also follow quite well a mass weighted calculation scheme according to Eq. (2) using the pure component values. For the measured viscosity a systematical negative deviation smaller than 2% from the prediction could be found as indicated by the drawn line in Fig. 4. The mixture data for the surface tension displayed in Fig. 5 show the tendency of a decreasing deviation from the prediction with decreasing distance from the critical point. These deviations from the prediction, however, are not larger than the measurement accuracy which is better than $\pm 0.2 \text{ mN}\cdot\text{m}^{-1}$, being partly limited by the available density data used for data evaluation. One must bear in mind that the quantity directly accessible in surface light scattering experiments is the ratio of the surface tension to the sum of the densities of the vapor and liquid phase. Thus reliable reference data for the densities under saturation conditions are needed. For the pure components R125 and R143a these were adopted from Refs. 24 and 25, respectively. Information about mixture densities was obtained with technical software from the manufacturer [26]. In a similar fashion as for the measurement of the surface tension, also the directly accessible quantity $\tilde{\mathbf{n}}$ obtained for the viscosity is determined by both the vapor and liquid properties, i.e.

$$\tilde{\mathbf{n}} = \frac{\mathbf{h}' + \mathbf{h}''}{\mathbf{r}' + \mathbf{r}''} \quad (3)$$

where \mathbf{h} and \mathbf{h}'' are the dynamic viscosities of the liquid and vapor phase, respectively, \mathbf{r}' and \mathbf{r}'' are the densities of the liquid and vapor phase. As appropriate reference data for vapor viscosities are not available which in particular is true for the mixtures, the approximation $\tilde{\mathbf{n}} \approx \mathbf{n}'$ has been used, which relies on the neglect of vapor

properties as compared with the respective liquid quantities, and thus yields an approximate kinematic liquid viscosity ν' . An estimation based on reference data indicates that for the fluids under investigation this approximation results in a deviation from the exact viscosity value of the liquid phase of about + 2% for temperatures below 300 K. For the highest temperature studied the systematic error caused by neglecting the influence of the vapor phase is increasing up to - 10%. However, excluding the highest temperatures studied in this work, the total uncertainty of our liquid viscosity data can be estimated to be better than $\pm 5\%$. For a more detailed discussion see Ref. 27.

3.2 Ternary Mixture R404A

For the ternary mixture ($T_C = 345.33$ K) the results of the thermal diffusivity and of the sound velocity are presented again in their dependence on the reduced temperature in Fig. 6 and 7, respectively. Here, besides those for R125 and R143a also the pure component data of R134a have to be taken into account in the correlation of the mixture data from those of the components. These R134a data have partly been measured in the frame of this research and partly been taken from former measurements [28]. They are represented by the dotted-dashed line in the figures. Again the measured mixture data can best be correlated by the mass weighted sum of the pure component properties, as given by Eq. (2), which is represented by the drawn line in the figures. From the deviation plots in Fig. 6 and 7 one can realize that the deviation is again smaller than 1% for the sound velocity and smaller than 5% for the thermal diffusivity for a reduced temperature up to 0.99.

In Fig. 8 and 9 the measured data of the liquid kinematic viscosity and of the surface tension, respectively, of R 404A are displayed. All different data sets of the

three pure components and of the mixture are represented by different symbols. For the evaluation of the surface tension of the additional component R134a, density values for the vapor and liquid phase were adopted from the equation of state of Tillner-Roth and Baehr [29]. The mixture densities are again calculated with the technical software from the manufacturer [26]. The predictions given by Eq. (2) for both quantities of the mixture are again indicated by the drawn lines in the figures. As can be seen from the deviation plot of Fig. 8, the proposed correlation of the mixture viscosities from the pure component data is in quite good agreement with the measured data for the entire temperature range studied in this work. For the surface tension of the ternary fluid mixture R404A the same statements regarding the mixture rule are valid as stated for the binary mixture.

4. CONCLUSION

We have shown for the first time that the DLS technique can also be applied successfully to the investigation of ternary fluid mixtures. Several thermophysical properties have been measured for the ternary mixture R404A and also for the binary mixture R507 which contains two components of the ternary mixture R404A. The experimental results suggest that the mixture data can best be represented by a mass weighted sum of the pure component data expressed as functions of the reduced temperature. This approach may also be useful for the prediction of properties of other refrigerant mixtures.

ACKNOWLEDGEMENTS

The investigated refrigerants have been provided by Solvay Fluor und Derivate GmbH, Hannover. Parts of the work were supported by the Deutsche Forschungsgemeinschaft (DFG).

REFERENCES

1. J. N. Shaumeyer, R.W. Gammon, and J. V. Sengers, in *Measurement of the Transport Properties of Fluids*, W. A. Wakeham, A. Nagashima, and J. V. Sengers, eds. (Blackwell Scientific, Oxford, 1991), pp. 197-213.
2. A. Leipertz, *Int. J. Thermophys.* **9**:897 (1988); *J. Chem. Eng.* **34**:188 (1994) and *Fluid Phase Equil.* **125**:219 (1996).
3. S. Will and A. Leipertz, in *Diffusion in Condensed Matter*, J. Kärger, P. Heitjans, and R. Haberlandt, eds. (Vieweg, Wiesbaden, 1999) pp. 219-244.
4. A. P. Fröba, S. Will, and A. Leipertz, *Fluid Phase Equil.* **161**:337 (1999).
5. M. Corti and V. Degiorgio, *J. Phys. C Solid State Phys.* **8**:953 (1975)
6. M. Hendrix, A. Leipertz, M. Fiebig, and G. Simonsohn, *Int. J. Heat Mass Transfer* **30**:333 (1987)
7. S. Will, A. P. Fröba, and A. Leipertz, *Int. J. Thermophys.* **19**:403 (1998).
8. E. Gulari, R. J. Brown, and C. J. Pings, *AIChE J.* **19**:1196 (1973)
9. G. Wu, M. Fiebig, and A. Leipertz, *Int. J. Heat Mass Transfer* **31**:1471 (1988) and **31**:2555 (1988).
10. H.-W. Fiedel, G. Schweiger, and K. Lucas, *J. Chem. Eng. Data* **36**:169 (1991).
11. G. Simonsohn, *Opt. Acta* **30**:875 (1983)

12. A. Leipertz, K. Kraft, and G. Simonsohn, *Fluid Phase Equil.* **79**:201 (1992).
13. K. Kraft and A. Leipertz, *Int. J. Thermophys.* **16**:445 (1995).
14. A. P. Fröba, S. Will, and A. Leipertz, *Appl. Opt.* **36**:7615 (1997).
15. S. Will and A. Leipertz, *Int. J. Thermophys.* **18**:1339 (1997)
16. S. Will and A. Leipertz, *Int. J. Thermophys.* **20**:791 (1999)
17. B. J. Ackerson and H. J. M. Hanley, *J. Chem. Phys.* **73**:3568 (1980).
18. J. W. Schmidt and M. R. Moldover, *J. Chem. Eng. Data* **39**:39 (1994).
19. J. W. Schmidt, E. Carrillo-Nava, and M. R. Moldover, *Fluid Phase Equil.* **122**:187 (1996).
20. J. Yata, M. Hori und T. Minamiyama, Refractive Index of HCFC-22 and HFC-
Proc. Jap. Symp. Thermophys. Prop. 11 / 1990, 111-114 (1990).
21. D. Langewin, *Light Scattering by Liquid Surfaces and Complementary
Techniques*, Marcel Dekker, New York, 1992.
22. K. Kraft and A. Leipertz, *Int. J. Thermophys.* 15:387 (1994).
23. A. P. Fröba, S. Will, and A. Leipertz, *Int. J. Thermophys.*, submitted (2000).
24. S. L. Outcalt and M. O. McLinden, *Int. J. Thermophys.* **16**:79 (1995).
25. K. Srinivasan and L. R. Oellrich, *Int. J. Refrig.* **20**:332 (1997).
26. Solvay Fluor & Derivate, SOLKANE[®] Refrigerant Software, Version 2.0
(1999).
27. A. P. Fröba, S. Will, and A. Leipertz, *Int. J. Thermophys.*, submitted (2000).
28. K. Kraft and A. Leipertz, *Fluid Phase Equil.* 125:245 (1996).
29. R. Tillner-Roth and H. D. Baehr, *J. Phys. Chem. Ref. Data* **23**:657 (1994).

FIGURE CAPTIONS

Fig. 1 Experimental setup: a) Optical and electronic arrangement b) Scattering geometry: light scattering by surface waves.

Fig. 2 Thermal diffusivity of the liquid (∇) and vapor phase (\blacktriangledown) under saturation conditions of the binary fluid mixture R507 as a function of the reduced temperature in comparison to a prediction (—) based on the quantities for the pure components R125 (·····) and R143a (— —).

Fig. 3 Sound velocity of the liquid (∇) and vapor phase (\blacktriangledown) under saturation conditions of the binary fluid mixture R507 as a function of the reduced temperature in comparison to a prediction (—) based on the quantities for the pure components R125 (·····) and R143a (— —).

Fig. 4 Kinematic viscosity of the liquid phase under saturation conditions of the binary fluid mixture R507 (\blacktriangledown) as a function of the reduced temperature in comparison to a prediction (—) based on the quantities for the pure components R125 (····· Δ) and R143a (— — \square).

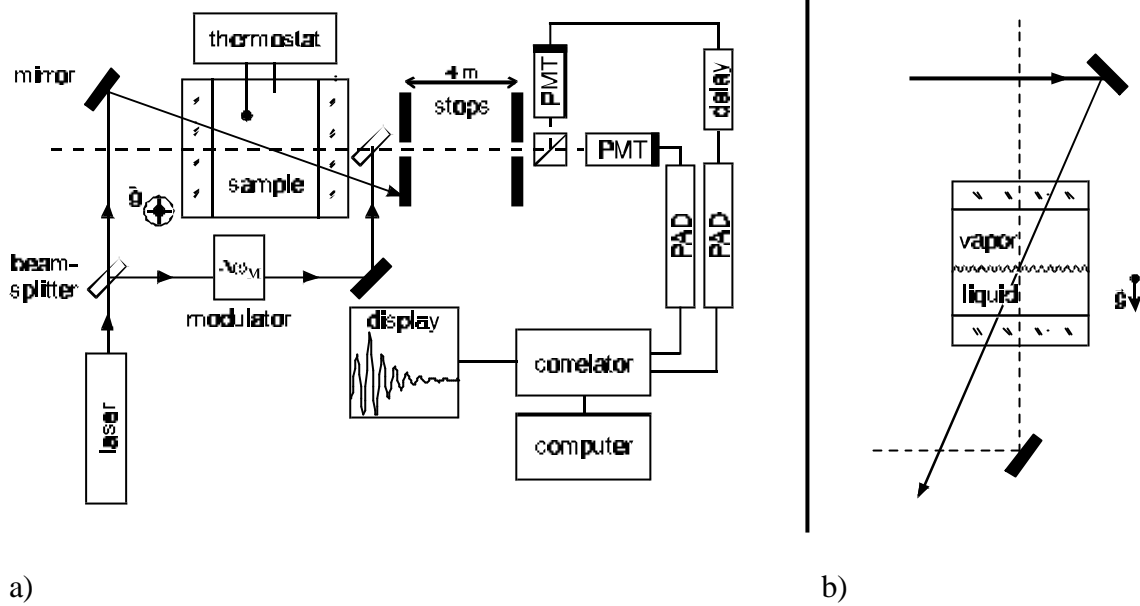
Fig. 5 Surface tension of the binary fluid mixture R507 (\blacktriangledown) as a function of the reduced temperature in comparison to a prediction (—) based on the quantities for the pure components R125 (····· Δ) and R143a (— — \square).

Fig. 6 Thermal diffusivity of the liquid (∇) and vapor phase (\blacktriangledown) under saturation conditions of the ternary fluid mixture R404A as a function of the reduced temperature in comparison to a prediction (—) based on the quantities for the pure components R125 (.....), R143a (— —), and R134a (— · —).

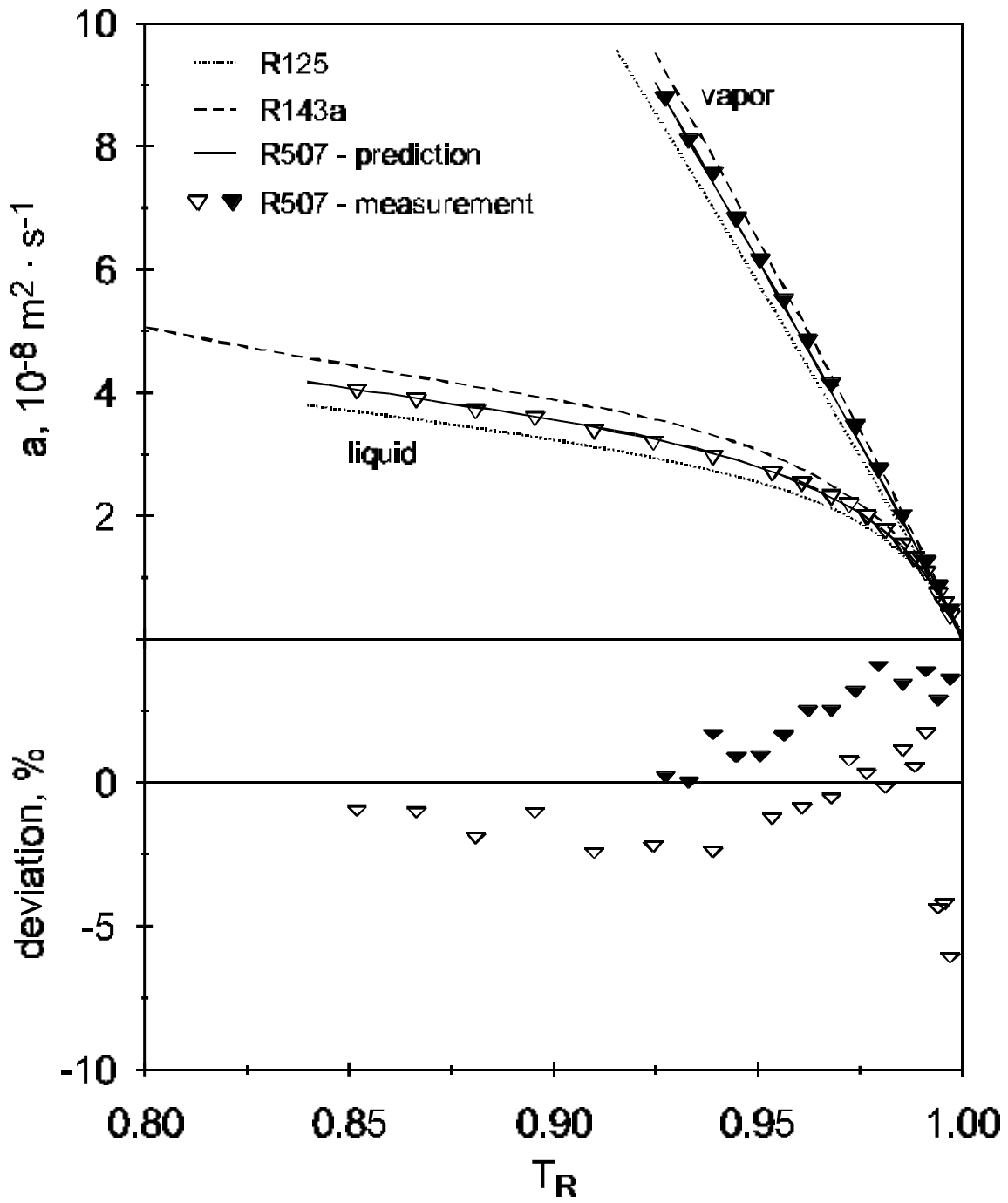
Fig. 7 Sound velocity of the liquid (∇) and vapor phase (\blacktriangledown) under saturation conditions of the ternary fluid mixture R404A as a function of the reduced temperature in comparison to a prediction (—) based on the quantities for the pure components R125 (.....), R143a (— —), and R134a (— · —).

Fig. 8 Kinematic viscosity of the liquid phase under saturation conditions of the ternary fluid mixture R404A (\blacktriangledown) as a function of the reduced temperature in comparison to a prediction (—) based on the quantities for the pure components R125 (..... Δ), R143a (— — \square), and R134a (— · — \oplus).

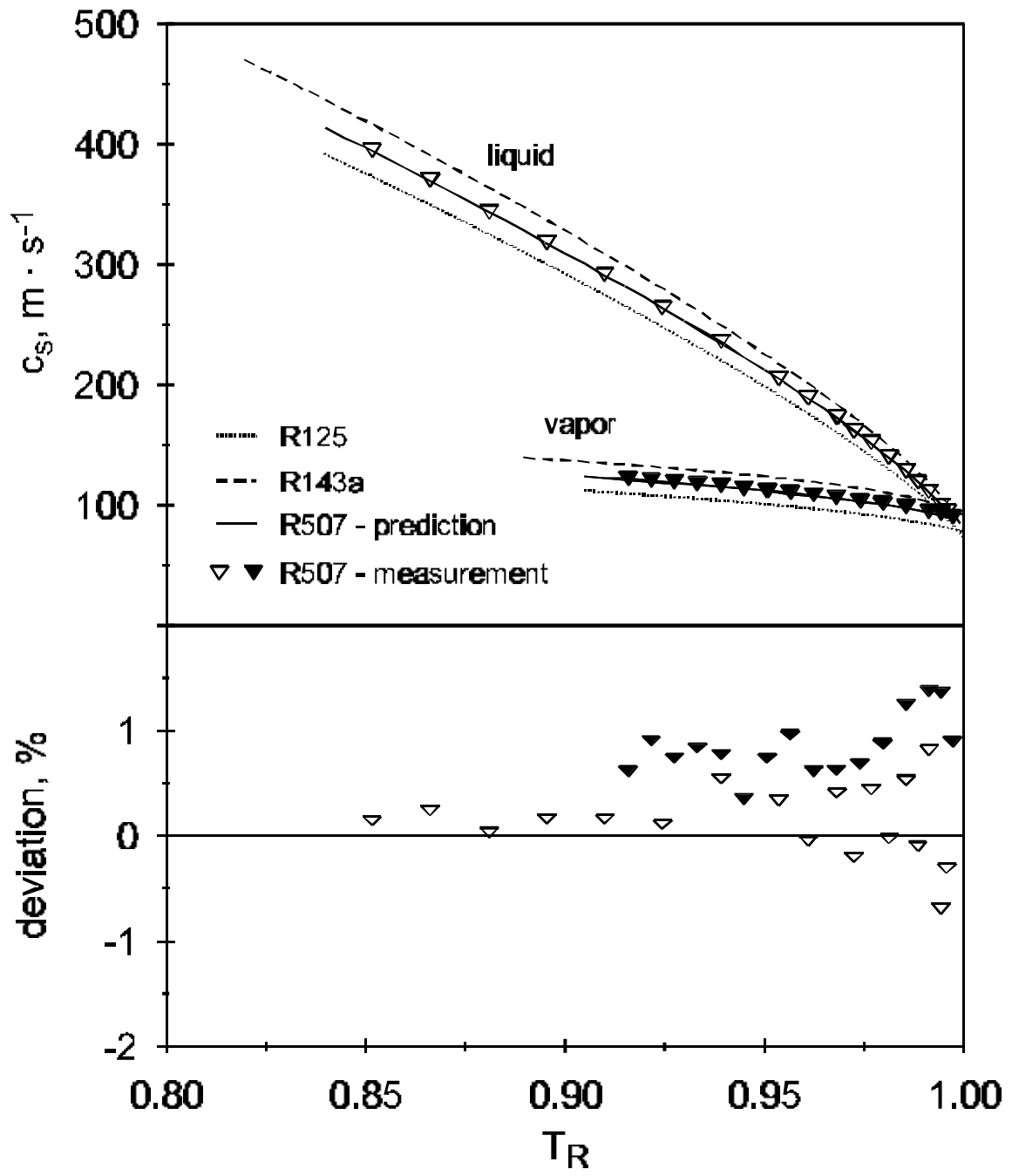
Fig. 9 Surface tension of the ternary fluid mixture R404A (\blacktriangledown) as a function of the reduced temperature in comparison to a prediction (—) based on the quantities for the pure components R125 (..... Δ), R143a (— — \square), and R134a (— · — \oplus).



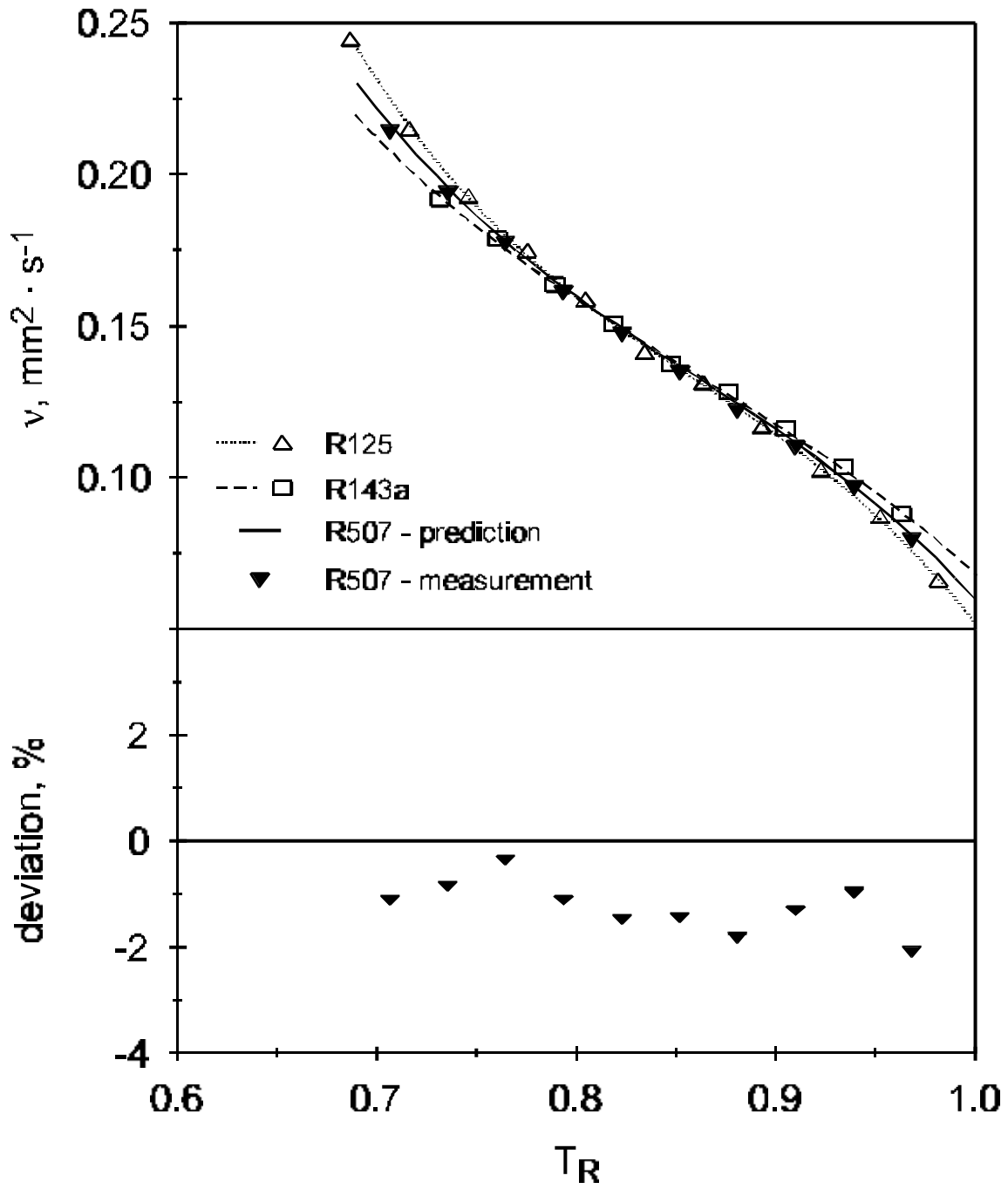
Fröba, Will, and Leipertz, Fig. 1



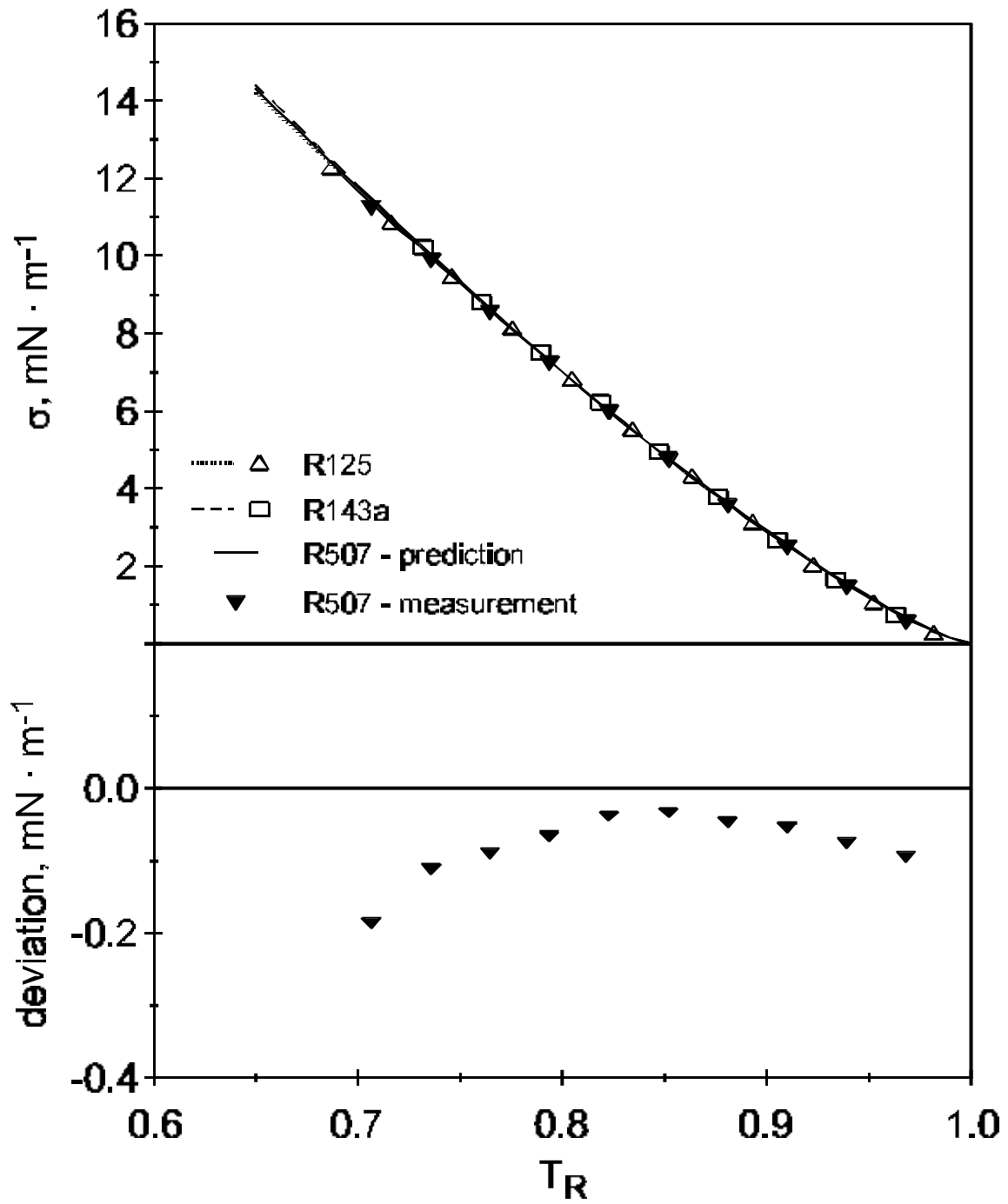
Fröba, Will, and Leipertz, Fig. 2



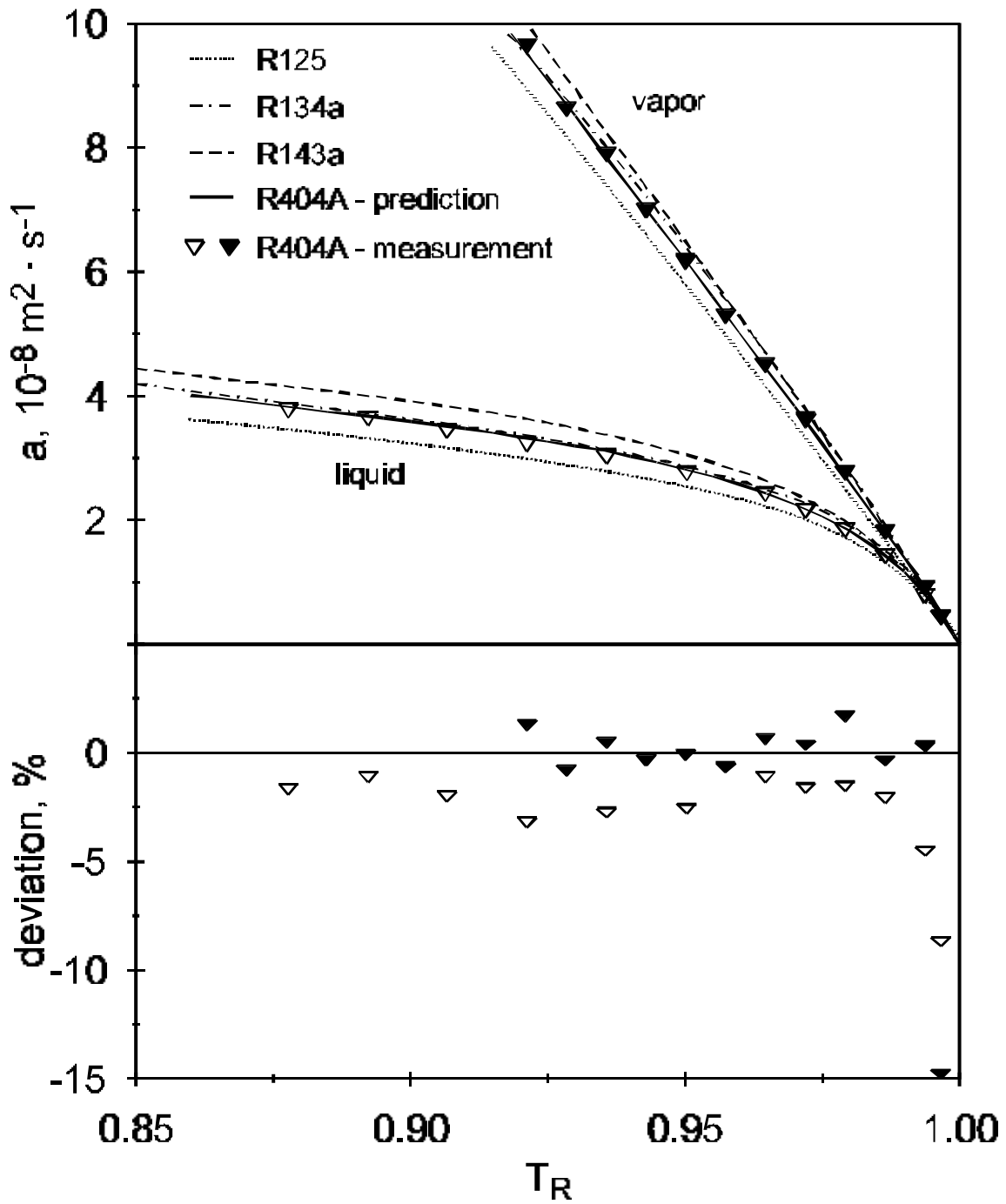
Fröba, Will, and Leipertz, Fig. 3



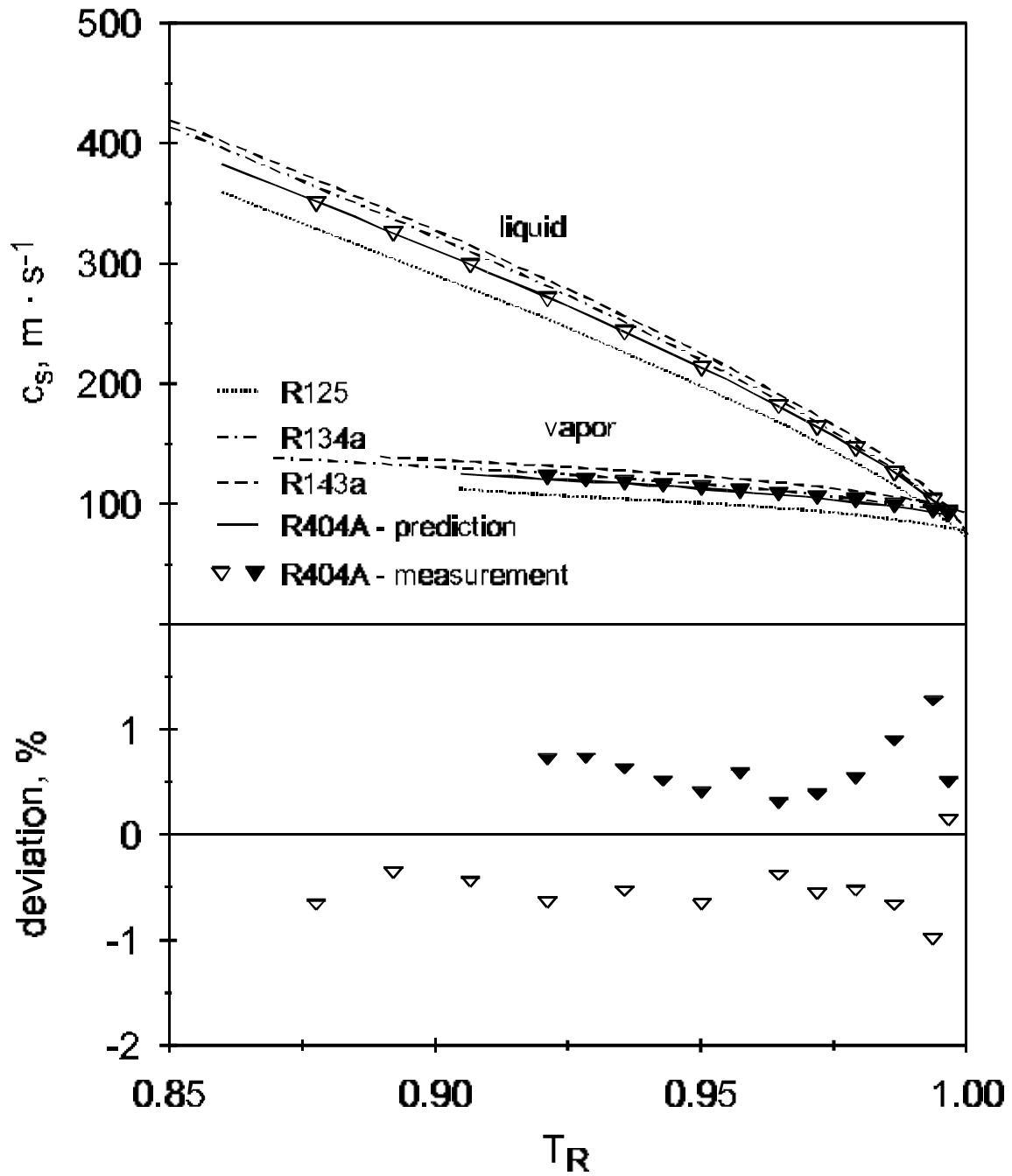
Fröba, Will, and Leipertz, Fig. 4



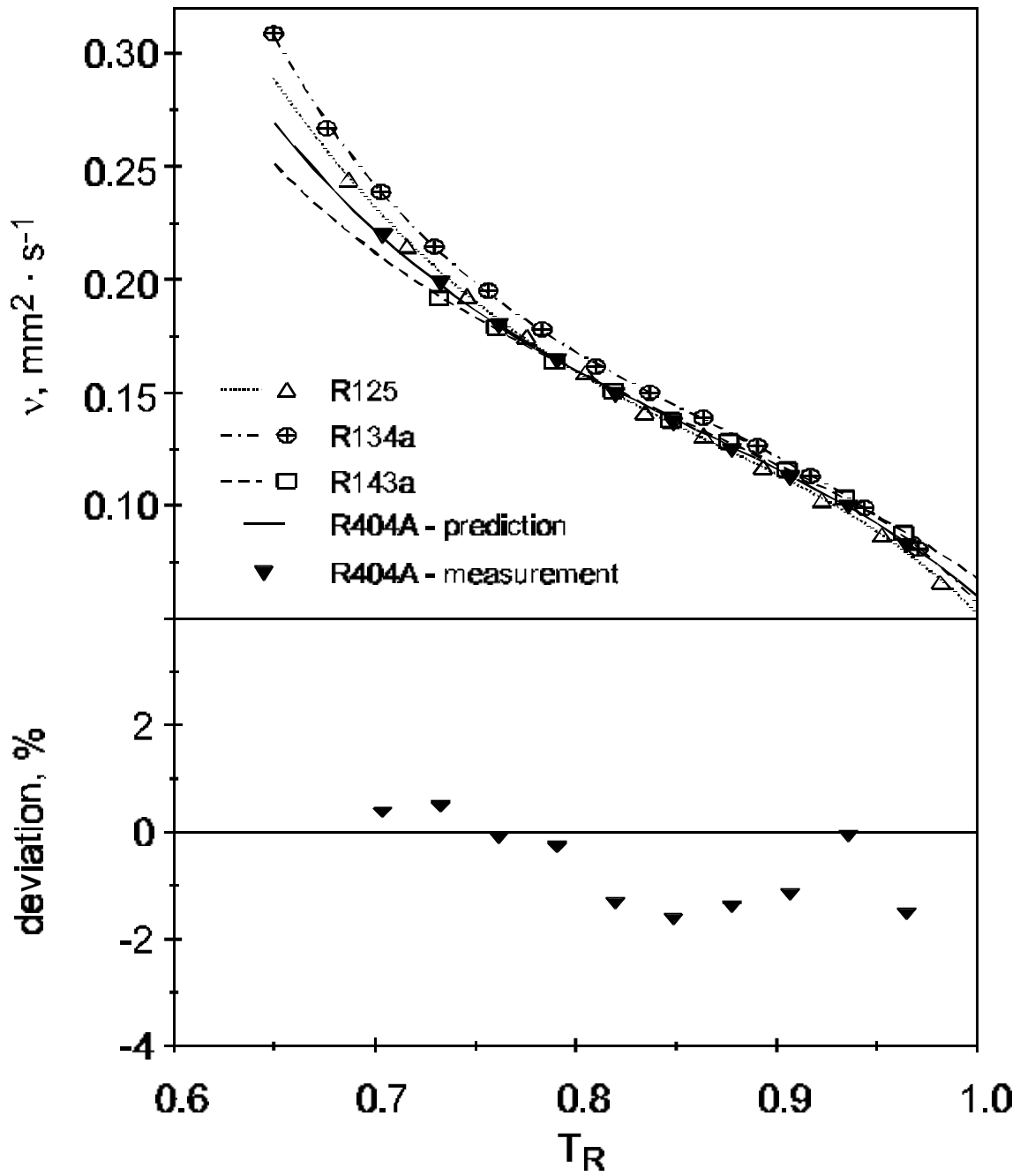
Fröba, Will, and Leipertz, Fig. 5



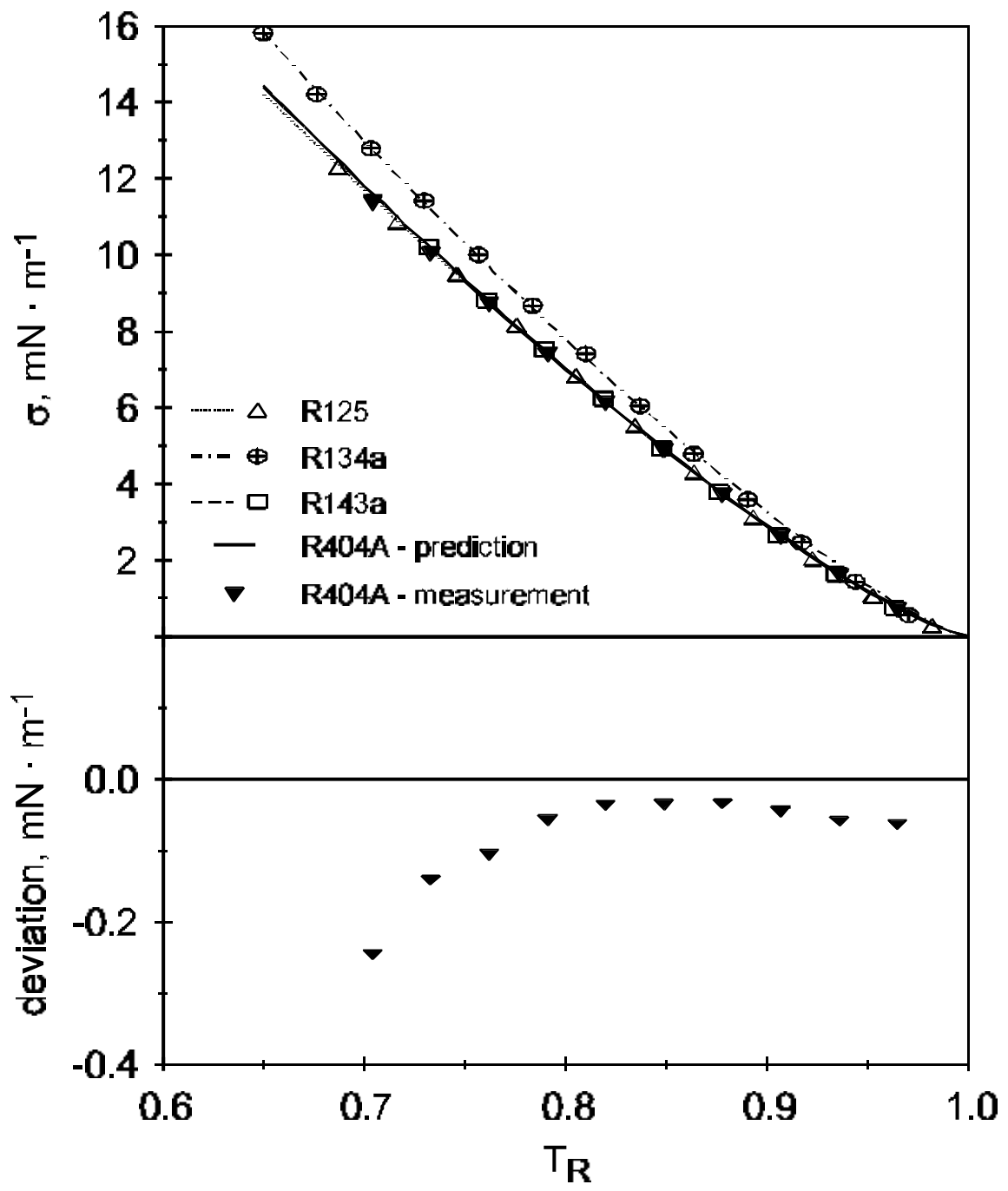
Fröba, Will, and Leipertz, Fig. 6



Fröba, Will, and Leipertz, Fig. 7



Fröba, Will, and Leipertz, Fig. 8



Fröba, Will, and Leipertz, Fig. 9